Ab-initio magneto-optical Kerr spectra

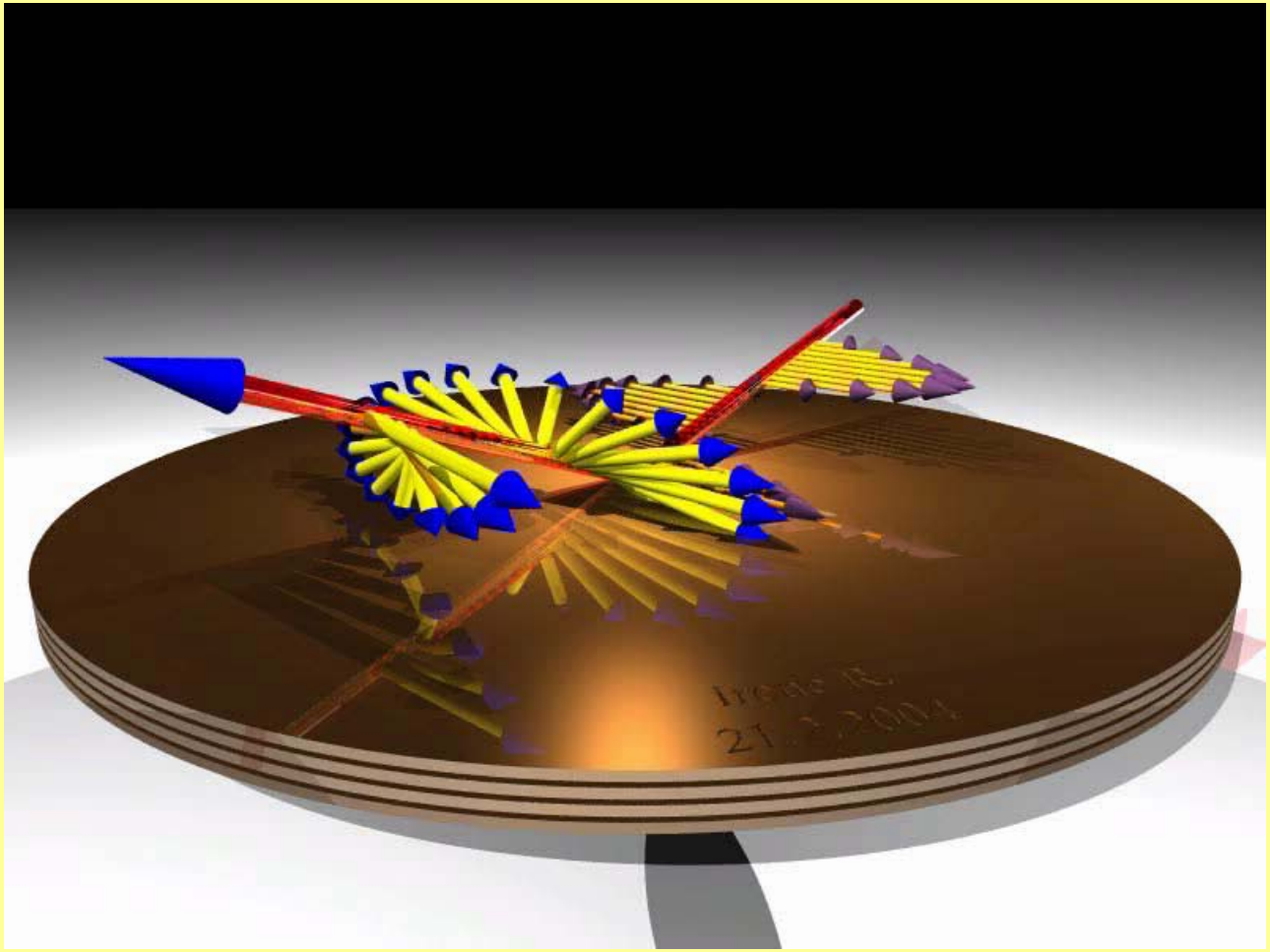

the two aspects:

- **Part I: the optical conductivity tensor – the quantum mechanical part**
- **Part II: evaluation of Kerr rotation and ellipticity angles including multiple interferences and reflexions – the classical optics part**

Part I : the optical conductivity tensor

J. Phys.: Condens. Matter **11** (1999) 10451–10458. Printed in the UK PII: S0953-8984(99)05241-8

Evaluation of the optical conductivity tensor in terms of contour integrations

László Szunyogh†‡ and Peter Weinberger‡

† Department of Theoretical Physics, Technical University of Budapest, Budafoki út 8, 1521 Budapest, Hungary

‡ Center for Computational Materials Science, Vienna, Getreidemarkt 9/158, 1060 Wien, Austria

Received 16 June 1999

Abstract. For the case of finite lifetime broadening the standard Kubo formula for the optical conductivity tensor is rederived in terms of Green's functions by using contour integrations, whereby finite temperatures are accounted for by using the Fermi–Dirac distribution function. For zero lifetime broadening, the present formalism is related to expressions well known in the literature. Numerical aspects of how to calculate the corresponding contour integrals are also outlined.

CMS

Within an independent-particle picture the interband part of the optical conductivity tensor at finite temperatures, $\Sigma_{\mu\nu}(\omega)$, is given by [1,3]

$$\Sigma_{\mu\nu}(\omega) = \frac{\bar{h}}{\mathrm{i}V} \sum_{m,n} \frac{f(\epsilon_n)(1 - f(\epsilon_m))}{\epsilon_n - \epsilon_m} \left\{ \frac{J^{\mu}_{nm} J^{\nu}_{mn}}{\bar{h}\omega + \epsilon_n - \epsilon_m + \mathrm{i}\delta} + \frac{J^{\nu}_{nm} J^{\mu}_{mn}}{\bar{h}\omega + \epsilon_m - \epsilon_n + \mathrm{i}\delta} \right\} \qquad (1)$$

where ω is the frequency, $f(\epsilon)$ is the Fermi function, V is the volume of the system and the $J^{\mu}_{nm} = \langle n | J^{\mu} | m \rangle$ are the matrix elements of the current-density operator J^{μ} ($\mu = x, y, z$) with respect to the eigenfunctions $|n\rangle$ of the one-electron Hamiltonian corresponding to energy eigenvalues ϵ_n. Lifetime-broadening effects due to different scattering processes are partially accounted for by a finite value of $\delta = \bar{h}/\tau \sim 0.03$ Ryd, where τ can be associated with a relaxation time [5,6]. Such a lifetime effect can be incorporated naturally into linear response theory either by assuming an adiabatic switching on of the external field $\phi(\boldsymbol{r}, t) = \phi(\boldsymbol{r})\mathrm{e}^{t/\tau}$ [8] or, equivalently, by convoluting the corresponding frequency-dependent conductivity for $\delta \to +0$ with a Lorentzian of finite halfwidth δ.

2. Contour integrations

Following Luttinger [8], equation (1) can be rewritten as

$$\Sigma_{\mu\nu}(\omega) = \frac{\sigma_{\mu\nu}(\zeta) - \sigma_{\mu\nu}(0)}{\zeta} \tag{2}$$

where $\zeta = \omega + \mathrm{i}\delta/\hbar$ and

$$\sigma_{\mu\nu}(\zeta) = \frac{\mathrm{i}}{V}\sum_{m,n}\frac{f(\epsilon_n) - f(\epsilon_m)}{\hbar\zeta + \epsilon_n - \epsilon_m} J^{\mu}_{nm} J^{\nu}_{mn}. \tag{3}$$

For simplicity, in what follows, we denote $\sigma_{\mu\nu}(\zeta)$ as $\sigma_{\mu\nu}(\omega)$ [11], in whose calculation we will be careful to keep it in mind that we have a finite imaginary part of the denominator in equation (3). Consider a pair of eigenvalues ϵ_n and ϵ_m. For a suitable contour $\mathcal{C}$ in the complex-energy plane (see figure 1) the residue theorem implies

$$\begin{aligned}\oint_{\mathcal{C}} \mathrm{d}z \, \frac{f(z)}{(z-\epsilon_n)(z-\epsilon_m+\hbar\omega+\mathrm{i}\delta)} \\ = -2\pi\mathrm{i}\frac{f(\epsilon_n)}{\epsilon_n - \epsilon_m + \hbar\omega + \mathrm{i}\delta} + 2\mathrm{i}\delta_T \sum_{k=-N_2+1}^{N_1} \frac{1}{(z_k - \epsilon_n)(z_k - \epsilon_m + \hbar\omega + \mathrm{i}\delta)}\end{aligned} \tag{4}$$

where the $z_k = \epsilon_F + \mathrm{i}(2k-1)\delta_T$ (ϵ_F is the Fermi energy, k_B the Boltzmann constant, T the temperature and $\delta_T = \pi k_B T$) are the so-called Matsubara poles. In equation (4) it was supposed that the N_1 and N_2 Matsubara poles in the upper and lower semi-plane lie within the contour $\mathcal{C}$, respectively, i.e.,

$$(2N_1 - 1)\delta_T < \delta_1 < (2N_1 + 1)\delta_T \tag{5}$$

$$(2N_2 - 1)\delta_T < \delta_2 < (2N_2 + 1)\delta_T. \tag{6}$$

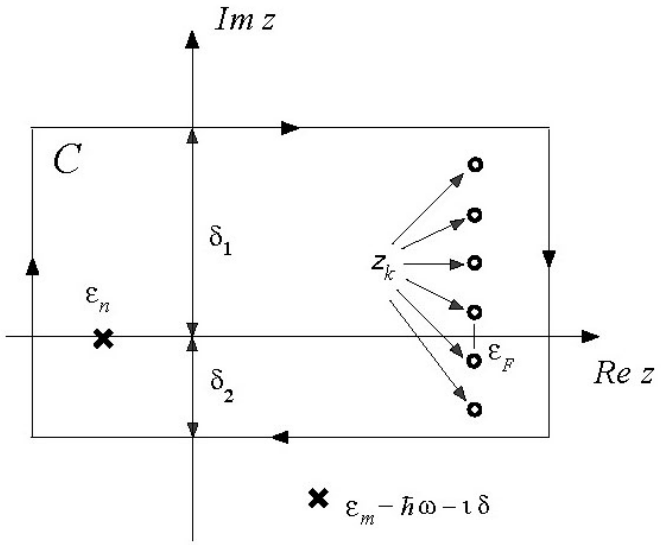

Figure 1. The contour in the complex plane corresponding to the integration in equation (4).

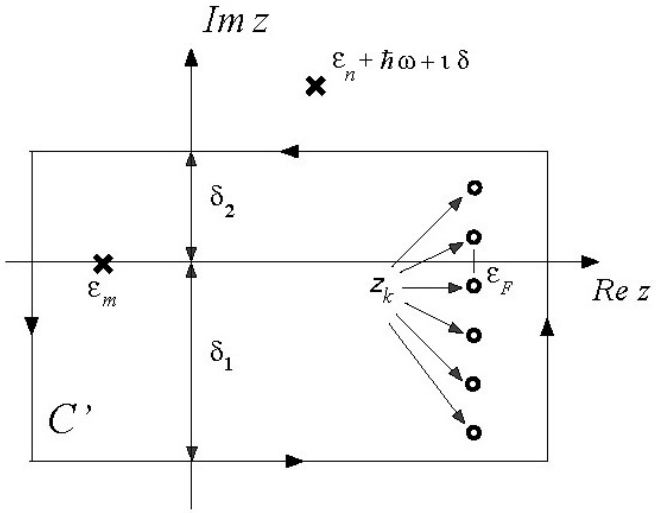

Figure 2. The contour in the complex plane corresponding to the integration in equation (8).

It is now straightforward to rewrite equation (9) in terms of the resolvent [12]:

$$G(z) = \sum_n \frac{|n\rangle\langle n|}{z - \epsilon_n} \tag{10}$$

such that

$$\begin{aligned}\sigma_{\mu\nu}(\omega) = -\frac{1}{2\pi V}\Bigg\{ & \oint_C \mathrm{d}z\ f(z)\,\mathrm{Tr}[J^\mu G(z+\bar{h}\omega+\mathrm{i}\delta)J^\nu G(z)] \\ & - \oint_{C'} \mathrm{d}z\ f(z)\,\mathrm{Tr}[J^\mu G(z)J^\nu G(z-\bar{h}\omega-\mathrm{i}\delta)]\Bigg\} \\ & + \mathrm{i}\frac{\delta_T}{\pi V}\Bigg\{ \sum_{k=-N_2+1}^{N_1} \mathrm{Tr}[J^\mu G(z_k+\bar{h}\omega+\mathrm{i}\delta)J^\nu G(z_k)] \\ & + \sum_{k=-N_1+1}^{N_2} \mathrm{Tr}[J^\mu G(z_k)J^\nu G(z_k-\bar{h}\omega-\mathrm{i}\delta)]\Bigg\}\end{aligned} \tag{11}$$

where Tr denotes the trace of an operator. By using the quantity given below, originally introduced by Butler [9]:

$$\widetilde{\sigma}_{\mu\nu}(z_1, z_2) = -\frac{1}{2\pi V}\,\mathrm{Tr}[J^\mu G(z_1)J^\nu G(z_2)] \tag{12}$$

for which the following symmetry relations apply:

$$\begin{aligned}&\widetilde{\sigma}_{\nu\mu}(z_2, z_1) = \widetilde{\sigma}_{\mu\nu}(z_1, z_2) \\ &\widetilde{\sigma}_{\mu\nu}(z_1^*, z_2^*) = \widetilde{\sigma}_{\nu\mu}(z_1, z_2)^* = \widetilde{\sigma}_{\mu\nu}(z_2, z_1)^*\end{aligned} \tag{13}$$

$\sigma_{\mu\nu}(\omega)$ can be written as

$$\begin{aligned}\sigma_{\mu\nu}(\omega) = & \oint_C \mathrm{d}z\ f(z)\widetilde{\sigma}_{\mu\nu}(z+\bar{h}\omega+\mathrm{i}\delta, z) - \oint_{C'} \mathrm{d}z\ f(z)\widetilde{\sigma}_{\mu\nu}(z, z-\bar{h}\omega-\mathrm{i}\delta) \\ & - 2\mathrm{i}\delta_T\Bigg\{ \sum_{k=-N_2+1}^{N_1} \widetilde{\sigma}_{\mu\nu}(z_k+\bar{h}\omega+\mathrm{i}\delta, z_k) + \sum_{k=-N_1+1}^{N_2} \widetilde{\sigma}_{\mu\nu}(z_k, z_k-\bar{h}\omega-\mathrm{i}\delta)\Bigg\}\end{aligned} \tag{14}$$

Green‘s functions:

CMS

Fully relativistic spin-polarized
Screened Korringa-Kohn-Rostoker method

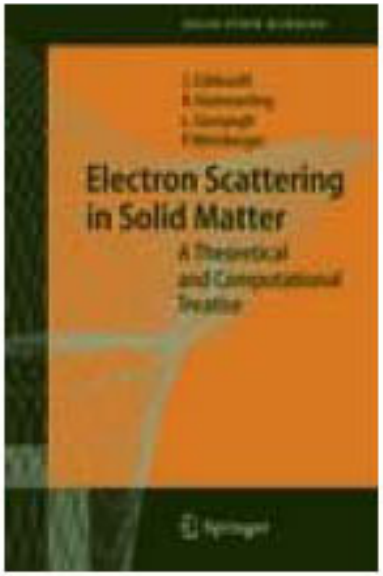

Electron Scattering in Solid Matter
A Theoretical and Computational Treatise
Series : Springer Series in Solid-State Sciences , Vol. 147
Zabloudil, J., **Hammerling**, R., **Szunyogh**, L., **Weinberger**, P.
2005, XV, 379 p. 89 illus., Hardcover
ISBN: 3-540-22524-2

Ready for shipping within 3 days.

A surprising view of optical conductivity

ELSEVIER

Journal of Magnetism and Magnetic Materials 240 (2002) 215–216

journal of magnetism and magnetic materials

www.elsevier.com/locate/jmmm

Layer-resolved optical conductivity of Co | Pt multilayers

A. Vernes[a], L. Szunyogh[a,b], L. Udvardi[a,b], P. Weinberger[a,*]

[a] *Center for Computational Materials Science, Technical University Vienna, Gumpendorferstr. 1a, 1060 Vienna, Austria*
[b] *Department of Theoretical Physics, Budapest University of Technology and Economics Budafoki út 8, 1521 Budapest, Hungary*

Abstract

The complex optical conductivity tensor is calculated for the Co | Pt multilayer systems by applying a contour integration technique within the framework of the spin-polarized relativistic screened Korringa–Kohn–Rostoker method. It is shown that the optical conductivity of the Co | Pt multilayer systems is dominated by contributions arising from the Pt cap and/or substrate layers.

Keywords: Conductivity tensor; Ferromagnetic multilayers; Green's function; Magneto-optics

Co/Pt(111)

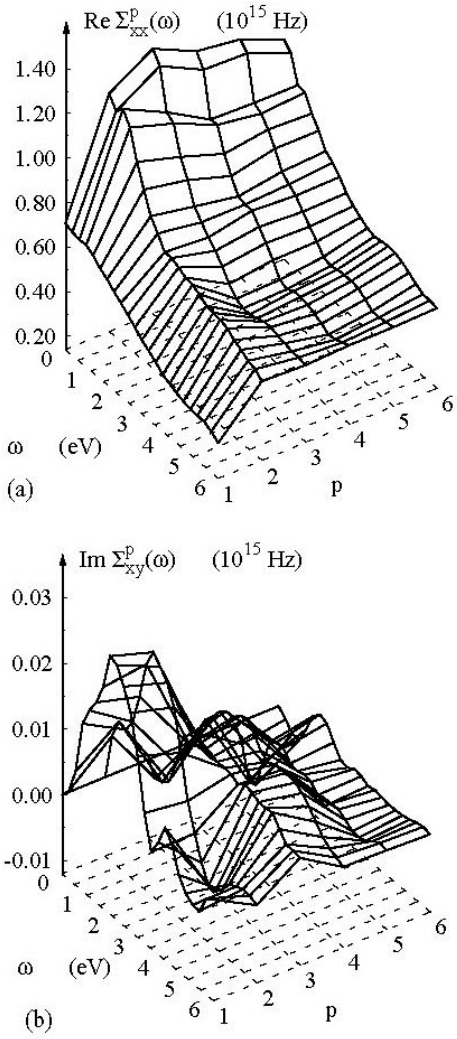

Fig. 1. Absorptive parts of the layer-resolved complex optical conductivity $\Sigma^p_{\mu\nu}(\omega)$ for FCC(1 1 1)–Co | Pt_5 as a function of the optical frequency ω and the layer index p. Heavy line marks the Co-layer resolved optical conductivity $\Sigma^{p-1}_{\mu\nu}(\omega)$.

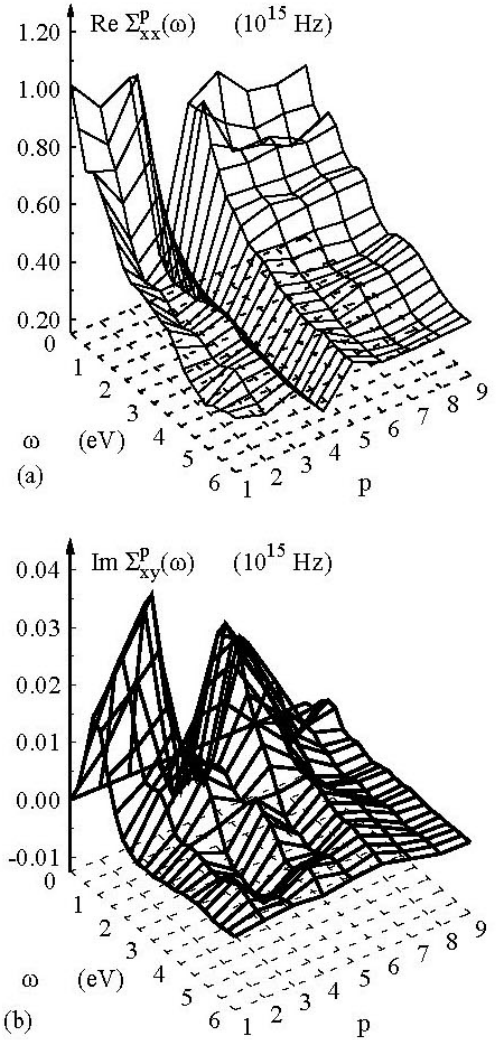

Fig. 2. Absorptive parts of the layer-resolved complex optical conductivity $\Sigma^p_{\mu\nu}(\omega)$ for FCC(1 1 1)–Pt_3 | Co | Pt_5 as a function of the optical frequency ω and the layer index p. Heavy line marks the Co-layer resolved optical conductivity $\Sigma^{p-1}_{\mu\nu}(\omega)$.

Part II: the two-media vs. a multimedia approach

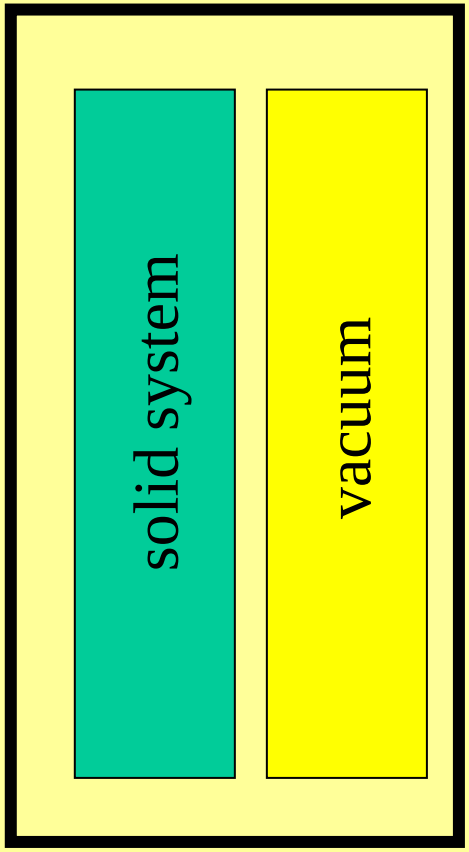

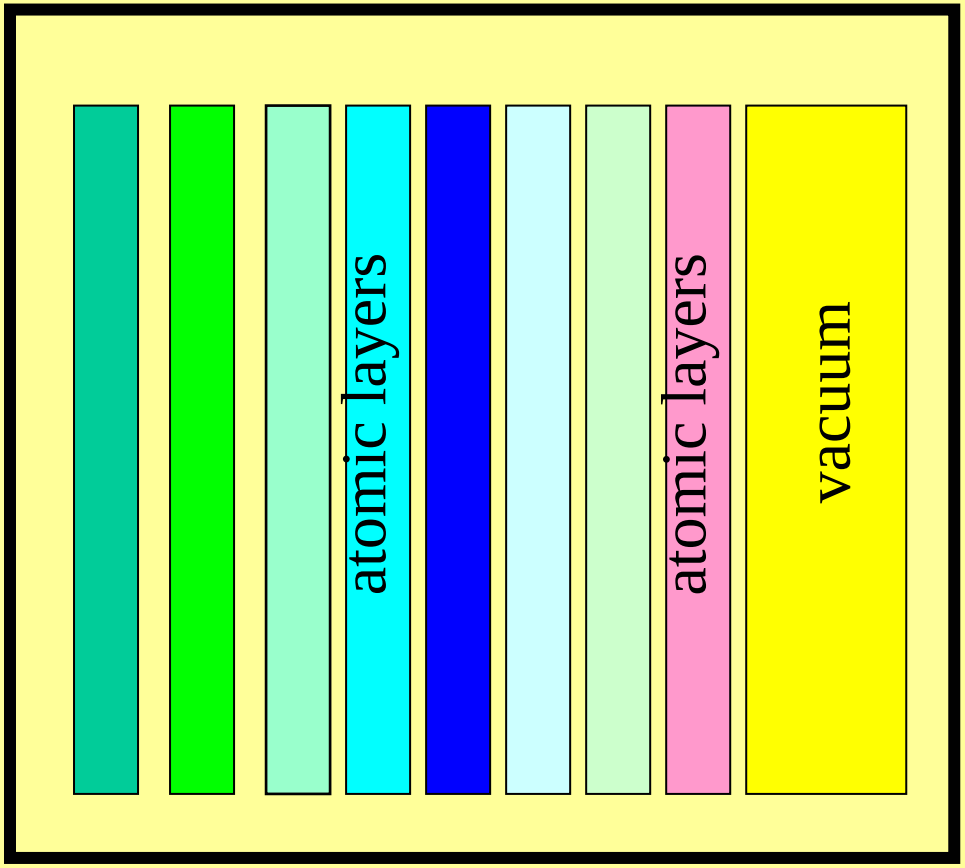

The multimedia approach:

PHYSICAL REVIEW B, VOLUME 65, 144448

Ab initio calculation of Kerr spectra for semi-infinite systems including multiple reflections and optical interferences

A. Vernes
Center for Computational Materials Science, Technical University Vienna, Gumpendorferstr. 1a, A-1060 Vienna, Austria

L. Szunyogh
Center for Computational Materials Science, Technical University Vienna, Gumpendorferstr. 1a, A-1060 Vienna, Austria
and Department of Theoretical Physics, Budapest University of Technology and Economics, Budafoki út 8, H-1521 Budapest, Hungary

P. Weinberger
Center for Computational Materials Science, Technical University Vienna, Gumpendorferstr. 1a, A-1060 Vienna, Austria
(Received 27 November 2001; published 4 April 2002)

Based on Luttinger's formulation the complex optical conductivity tensor is calculated within the framework of the spin-polarized relativistic screened Korringa-Kohn-Rostoker method for layered systems by means of a contour integration technique. For polar geometry and normal incidence, *ab initio* Kerr spectra of multilayer systems are then obtained by including via a 2×2 matrix technique all multiple reflections between layers and optical interferences in the layers. Applications to Co/Pt_5 and $Pt_3/Co/Pt_5$ on the top of a semi-infinite fcc(111) Pt bulk substrate show a good qualitative agreement with the experimental spectra, but differ from those obtained by applying the commonly used two-media approach.

DOI: 10.1103/PhysRevB.65.144448 PACS number(s): 75.50.Ss, 71.15.Rf, 78.20.Ls, 78.66.Bz

In the case of the polar magneto-optical Kerr effect (PMOKE),[14] the Kerr rotation angle

$$\theta_K = -\frac{1}{2}(\Delta_+ - \Delta_-) \tag{9}$$

and the Kerr ellipticity

$$\varepsilon_K = -\frac{r_+ - r_-}{r_+ + r_-} \tag{10}$$

are given in terms of the complex reflectivity of the right- (+) and left-handed (–) circularly polarized light:

$$\tilde{r}_\pm = \frac{\mathcal{E}_\pm^{(r)}}{\mathcal{E}^{(i)}} = r_\pm e^{i\Delta_\pm}. \tag{11}$$

Here the complex amplitude of the reflected right- and left-handed circularly polarized light is denoted by $\mathcal{E}_\pm^{(r)}$, and that of the incident light by $\mathcal{E}^{(i)}$; $\Delta_\pm$ is the phase of the complex reflectivity $\tilde{r}_\pm$ and $r_\pm = |\tilde{r}_\pm|$. Equations (9) and (10) are exact, which can easily be deduced from simple geometrical arguments. However, in order to apply these relations, one needs to make use of a macroscopic model for the occurring reflectivities.

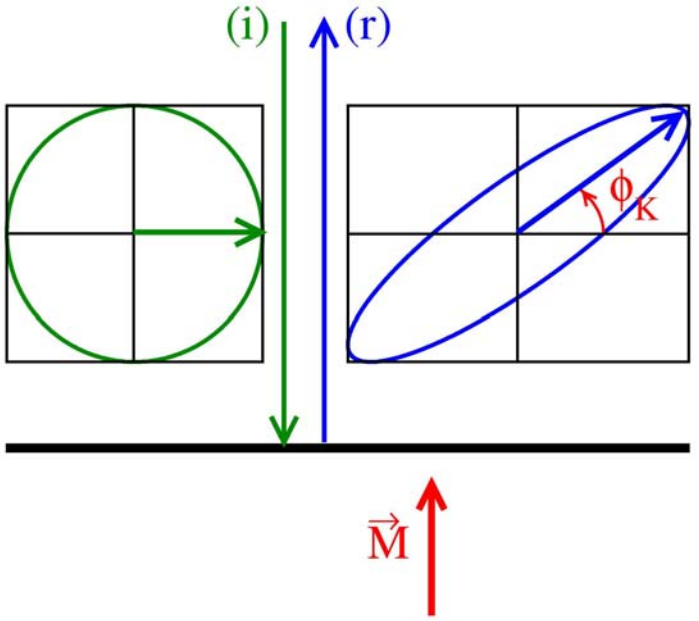

By mapping the interlayer and intralayer contributions $\tilde{\boldsymbol{\sigma}}^{pq}(\omega)$ to the microscopically exact optical conductivity tensor $\tilde{\boldsymbol{\sigma}}(\omega)$ [Eq. (6)], onto the corresponding contributions of the permittivity tensor,

$$\tilde{\boldsymbol{\epsilon}}^{pq}(\omega) = \frac{1}{N}\left[1 + \frac{4\pi i}{\omega}\tilde{\boldsymbol{\sigma}}^{pq}(\omega)\right], \tag{19}$$

one then can establish a well-defined macroscopical model for the evaluation of Kerr spectra.

As a first step the Fresnel or characteristic equation[40]

$$|\tilde{n}_p^2\delta_{\mu\nu}-\tilde{n}_{p\mu}\tilde{n}_{p\nu}-\tilde{\epsilon}^p_{\mu\nu}|=0 \quad (\mu,\nu=x,y,z) \tag{20}$$

has to be solved in order to determine the normal modes of the electromagnetic waves in a particular layer p.[41] Then by solving the Helmholtz equation for each normal mode,[41]

$$\sum_\nu (\tilde{n}_p^2\delta_{\mu\nu}-\tilde{n}_{p\mu}\tilde{n}_{p\nu}-\tilde{\epsilon}^p_{\mu\nu})\mathcal{E}_{p\nu}=0 \quad (\mu,\nu=x,y,z), \tag{21}$$

the corresponding $\mathcal{E}_{p\nu}$ components of the electric field in layer p are deduced. After having obtained the $\mathcal{E}_{p\nu}$s, the curl Maxwell equation[18,19]

$$\vec{\mathcal{H}}_p=\vec{n}_p\times\vec{\mathcal{E}}_p \tag{22}$$

provides the amplitudes of the magnetic fields $\vec{\mathcal{H}}_p$ for each normal mode in layer p. Here the Gaussian system of units has been used, $\vec{n}_p$ is the refraction vector, as given by Eq. (16), and $|\vec{n}_p|=\tilde{n}_p$, which in an anisotropic medium is direction and frequency dependent.[40]

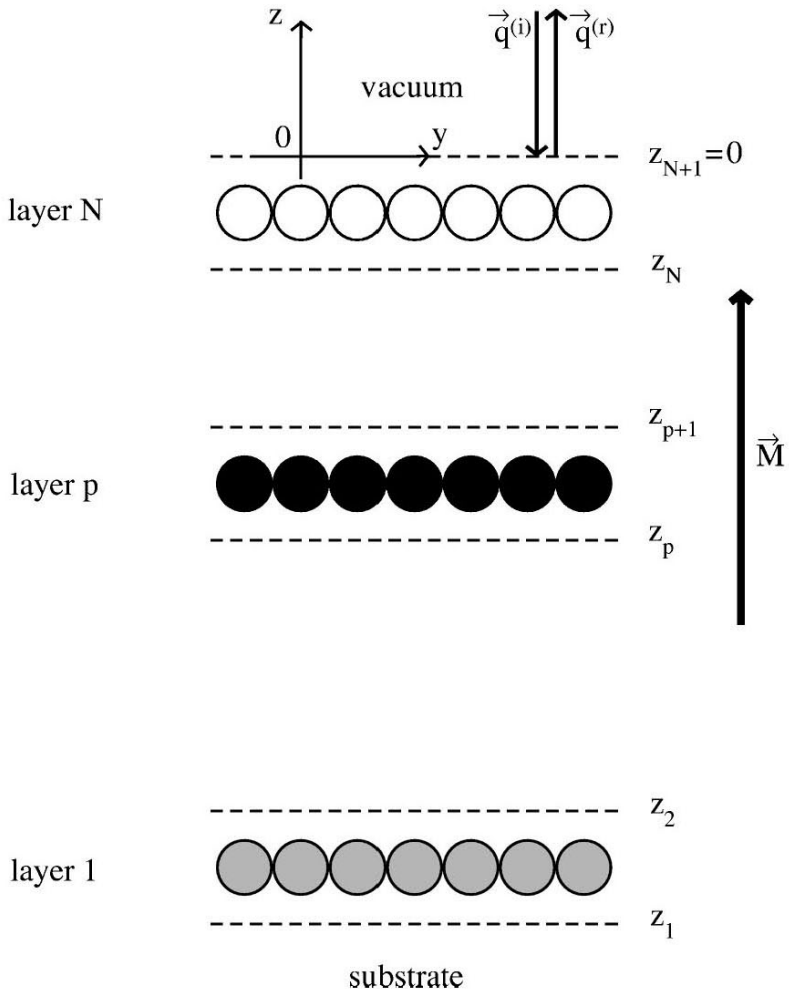

FIG. 1. The macroscopic model used for a layered system within the 2×2 matrix technique for polar geometry and normal incidence. The x axis is perpendicular to the plane of the figure, $\vec{q}^{(i)}$ is the incident wave vector and $\vec{q}^{(r)}$ is the reflected wave vector. $\vec{M}$ denotes the total spontaneous magnetization of the system.

For details of the 2 x 2 matrix technique see also

PHYSICAL REVIEW B **66**, 214404 (2002)

Limitations of the two-media approach in calculating magneto-optical properties of layered systems

A. Vernes
Center for Computational Materials Science, Technical University Vienna, Gumpendorferstr. 1a, A–1060 Vienna, Austria

L. Szunyogh
Center for Computational Materials Science, Technical University Vienna, Gumpendorferstr. 1a, A–1060 Vienna, Austria and Department of Theoretical Physics, Budapest University of Technology and Economics, Budafoki út 8, H–1521 Budapest, Hungary

P. Weinberger
Center for Computational Materials Science, Technical University Vienna, Gumpendorferstr. 1a, A–1060 Vienna, Austria
(Received 27 June 2002; published 5 December 2002)

It is shown that in polar geometry and normal incidence the 2×2 matrix technique—as discussed in detail in a preceding paper [Phys. Rev. B **65**, 144448 (2002)]—accounts correctly for multiple reflections and optical interferences, and reduces only in the case of a periodic sequence of identical layers to the Fresnel formula of reflectivity, which in turn is the theoretical basis of the two-media approach, widely used in the literature to compute magneto–optical Kerr spectra. As a numerical example *ab initio* calculations of the optical constants for an fcc Pt semi-infinite bulk using the spin-polarized relativistic screened Korringa-Kohn-Rostoker method show very good agreement with experimental data.

DOI: 10.1103/PhysRevB.66.214404 PACS number(s): 78.20.Bh, 78.20.Ci, 78.20.Ls

Fe/Pd(100) #1

PHYSICAL REVIEW B **70**, 195407 (2004)

Longitudinal Kerr effect in ultrathin Fe films on Pd(100)

A. Vernes, I. Reichl, and P. Weinberger
Center for Computational Materials Science, Technical University Vienna, Gumpendorferstrasse 1a, A-1060 Vienna, Austria

L. Szunyogh
Center for Computational Materials Science, Technical University Vienna, Gumpendorferstrasse 1a, A-1060 Vienna, Austria and Department of Theoretical Physics, University of Technology and Economics, Budafoki út 8, H-1521 Budapest, Hungary

C. Sommers
Laboratoire de Physique des Solides, Université de Paris-Sud, F-91405 Orsay, France
(Received 4 June 2004; published 10 November 2004)

Based on Luttinger's formulation the complex optical conductivity tensor of ultrathin films of Fe on Pd(100) is calculated by means of the spin-polarized relativistic screened Korringa-Kohn-Rostoker method using a contour integration technique. For longitudinal geometry and oblique incidence *ab initio* Kerr spectra are then obtained via a 2×2 matrix technique that takes into account all multiple reflections between layers and optical interferences. The obtained results are in very good agreement with the available experimental data.

DOI: 10.1103/PhysRevB.70.195407 PACS number(s): 78.20.Ls, 71.15.Rf, 78.66.Bz, 78.67.Pt

Fe/Pd(100) #2

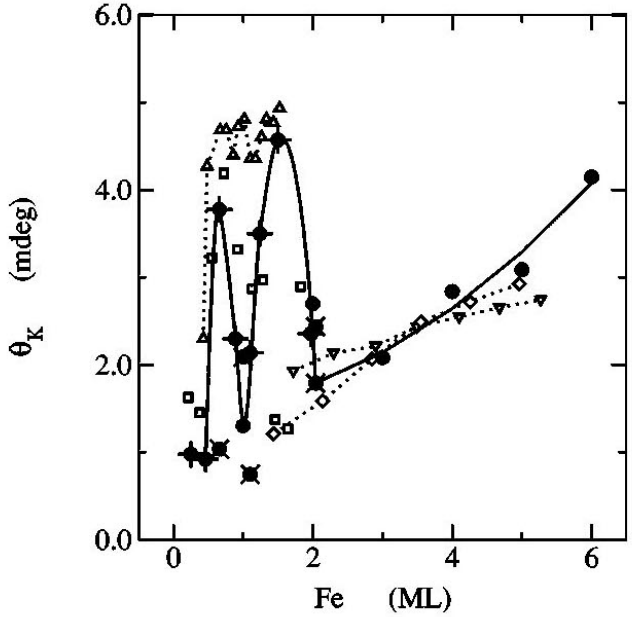

FIG. 1. Longitudinal Kerr rotation angle for oblique incidence (θ=70°) and p-polarized light ($\hbar\omega$=1.847 654 eV) in the case of fcc Fe/Pd(100). The calculated Kerr rotation angles θ_K in mdeg (10^{-3} deg) corresponding to concentration profiles I (II) are shown as pluses (crosses) and those corresponding to the ordered layered systems Fe_N/Pd(100), with $N \in \mathbb{N}$, as solid circles. The properly scaled experimental Kerr signals (arbitrary units) from Ref. 3 refer to open symbols: squares, up and down triangles denote data from samples obtained by pulse laser deposition performed at temperatures T=50–70 K, while diamonds represent data recorded from thermal deposited probes at room temperature. Dashed lines connect different experimental Kerr signal sets; the solid line follows the regression of the calculated Kerr rotation angles for concentration profiles I and for the ordered layered systems.

CMS

Cu/Ni/Cu/Ni/Cu(100) #1

PHYSICAL REVIEW B **70**, 214417 (2004)

Ab initio determination of Kerr angles in $Cu_4Ni_8Cu_nNi_9/Cu(100)$ ($n=2-10$)

I. Reichl, R. Hammerling, A. Vernes, and P. Weinberger
Center for Computational Material Science, Vienna University of Technology, Getreidemarkt 9/134, A-1060 Vienna, Austria

C. Sommers
Laboratoire de Physique des Solides, Université de Paris-Sud 91405 Orsay Cedex, France

L. Szunyogh
Center for Computational Material Science, Vienna University of Technology, Getreidemarkt 9/134, A-1060 Vienna, Austria and Department of Theoretical Physics and Center for Applied Mathematics and Computational Physics, Budapest University of Technology and Economics, Budafoki út 8, H-1521 Budapest, Hungary
(Received 12 August 2004; published 17 December 2004)

Calculated polar magneto-optic Kerr rotation and ellipticity angles are presented for the system $Cu_4Ni_8Cu_nNi_9/Cu(100)$, $n=2,\ldots,10$. Contrary to the common belief, the Kerr signals are found to be not directly proportional to the total magnetic moment. It will be shown that in order to assign at least indirectly the size (and sign) of the Kerr angles and therefore the type of coupling to a kind of total magnetic moment, one has to consider weighted layer-resolved moments, e.g., weighted by the damping factors of the reflected waves. As to be expected the occurring oscillations in the Kerr angles with respect to the spacer thickness resemble closely those for the interlayer exchange coupling energy.

DOI: 10.1103/PhysRevB.70.214417 PACS number(s): 77.22.Ch, 78.20.Bh, 78.20.Ci, 78.20.Ls

Cu/Ni/Cu/Ni/Cu(100) #2

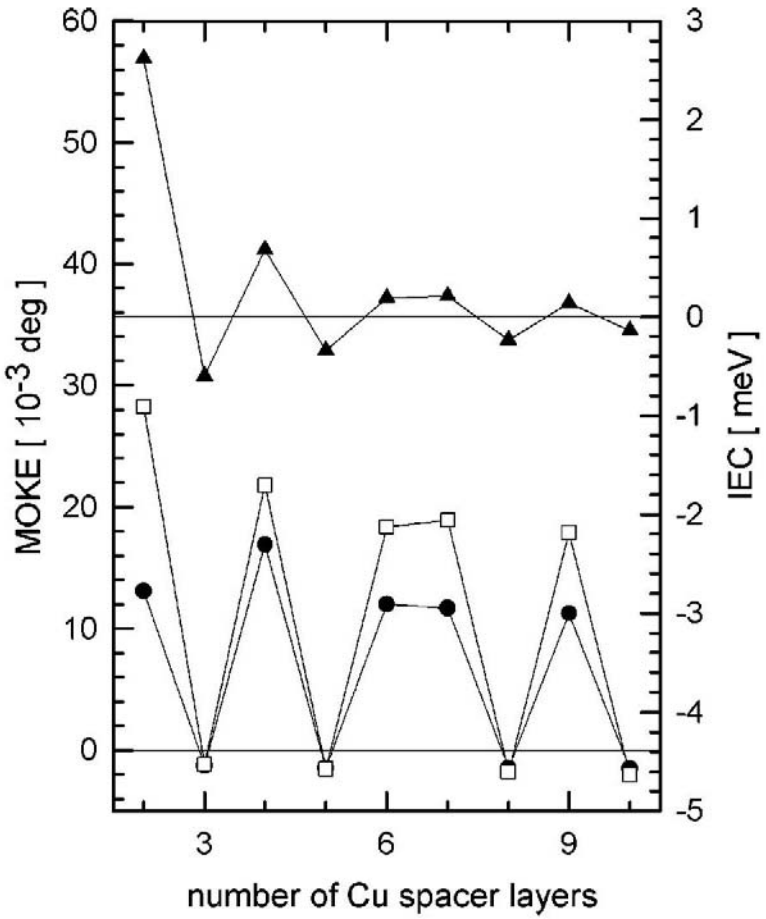

FIG. 3. Comparison between IEC and MOKE for $Cu_4Ni_8Cu_nNi_9/Cu(100)$ with respect to the number of Cu spacer layers. Triangles denote the theoretical IEC results of Ref. 1, circles and squares the calculated Kerr angles θ_K and ε_K, respectively.

Cu/Ni/Cu/Ni/Cu(100) #3

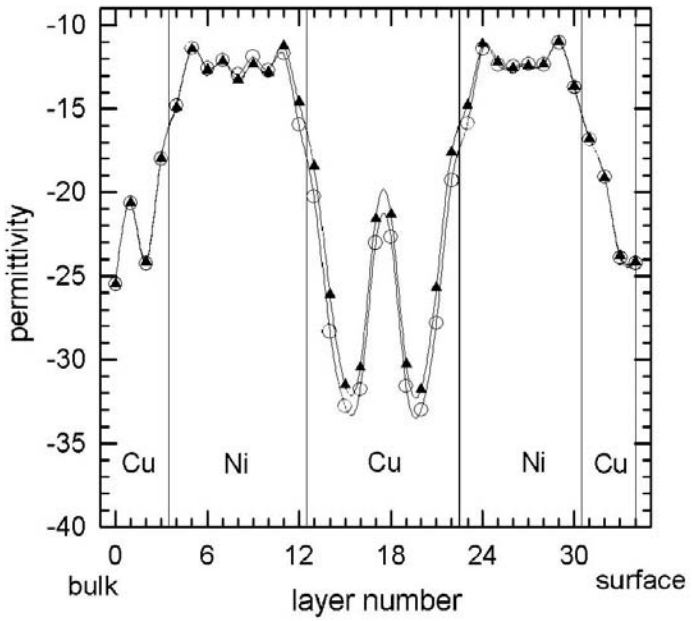

FIG. 4. Comparison of the AFM (triangles) and FM (circles) layer-resolved complex permittivity $\mathrm{Re}(\varepsilon_{xx})$ for $Cu_4Ni_8Cu_{10}Ni_9/Cu(100)$.

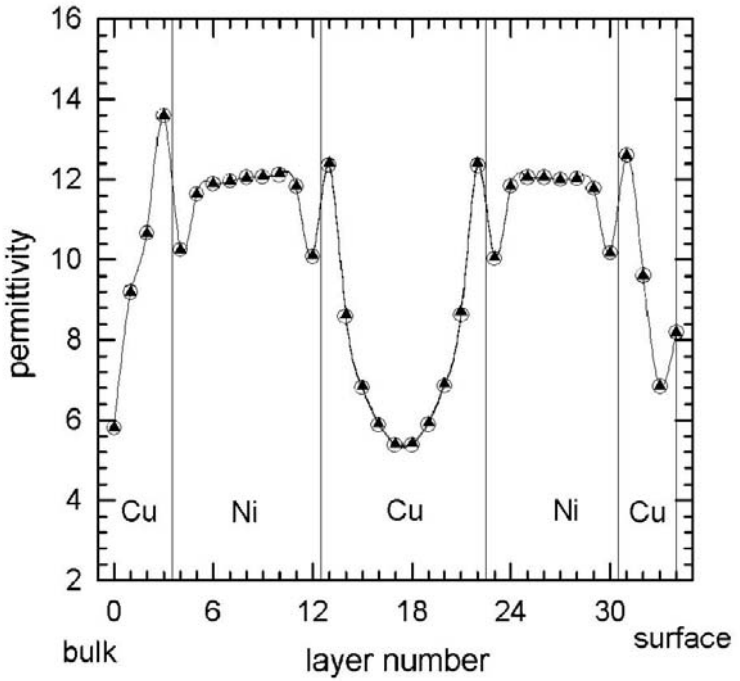

FIG. 5. Comparison of the AFM (triangles) and FM (circles) layer-resolved complex permittivity $\mathrm{Im}(\varepsilon_{xx})$ for $Cu_4Ni_8Cu_{10}Ni_9/Cu(100)$.

Cu/Ni/Cu/Ni/Cu(100) #4

PHYSICAL REVIEW B **70**, 214417 (2004)

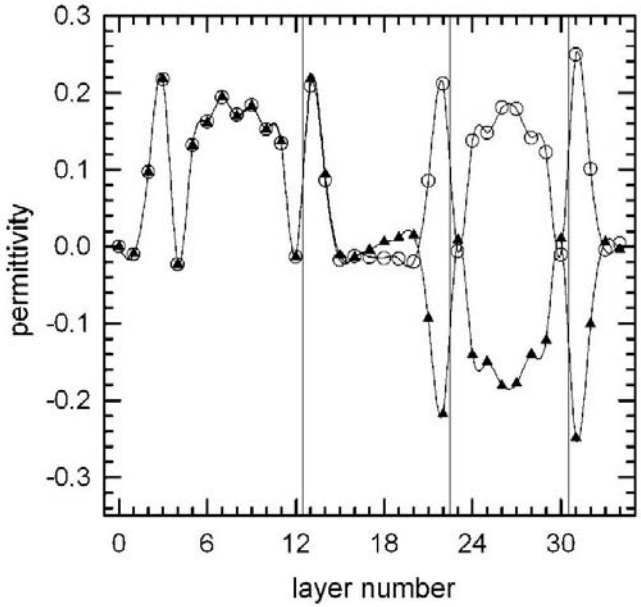

FIG. 8. Comparison of the AFM (triangles) and FM (circles) layer-resolved complex permittivity $\mathrm{Re}(\varepsilon_{xy})$ for $Cu_4Ni_8Cu_{10}Ni_9/Cu(100)$.

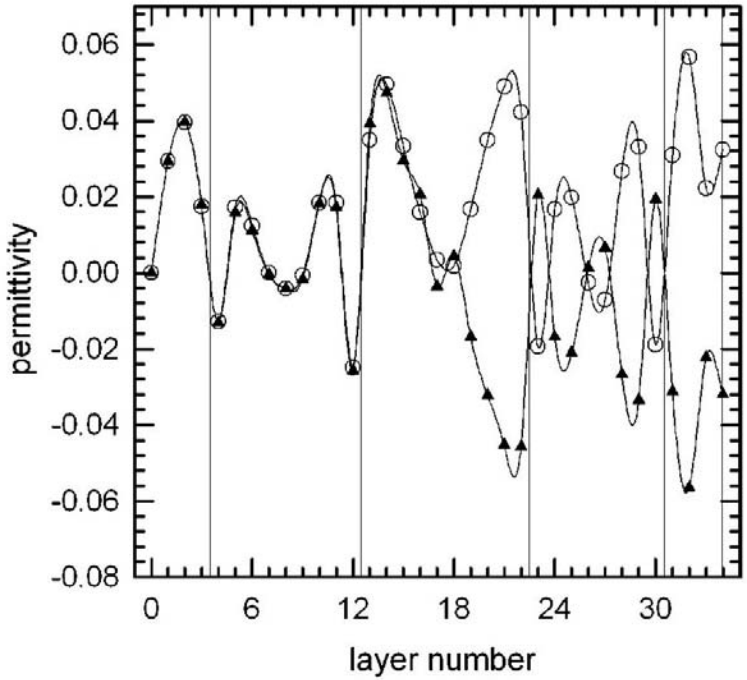

FIG. 9. Comparison of the AFM (triangles) and FM (circles) layer-resolved complex permittivity $\mathrm{Im}(\varepsilon_{xy})$ for $Cu_4Ni_8Cu_{10}Ni_9/Cu(100)$.

Fe/Au(100): the reorientation transition

Phys. Rev. B **71**, 214416/1-5 (2005)

The reorientation transition in Fe_n/Au(100)

I. Reichl, A. Vernes and P. Weinberger
Center for Computational Materials Science, Vienna University of Technology, Gumpendorferstr. 1a, A-1060 Vienna, Austria

L. Szunyogh
Department of Theoretical Physics and Center for Applied Mathematics and Computational Physics, Budapest University of Technology and Economics, Budafoki út 8, H-1521 Budapest, Hungary and Center for Computational Materials Science, Vienna University of Technology, Gumpendorferstr. 1a, A-1060 Vienna, Austria

C. Sommers
Laboratoire de Physique des Solides, Université de Paris-Sud 91405 Orsay Cedex, France
(Dated: February 3, 2005)

Experimental investigations and theoretical magnetic anisotropy energy calculations show a reorientation transition of the magnetization in Fe_n/Au(100) from a normal-to-plane to an in-plane direction at about 3 monolayers of Fe. In the present paper the magneto-optical properties of this system are investigated theoretically by using the spin-polarized relativistic screened Korringa-Kohn-Rostoker method, the Kubo-Greenwood equation for finite photon frequencies and a classical optical approach that takes into account all reflections and interferences. By varying the thickness of the Fe film, the reorientation of the ground-state magnetization is clearly traced as a strong decrease in the calculated Kerr rotation angles for oblique incidence of light. For all film thicknesses under consideration, it is found that by continuously varying the angle of the incident light the Kerr rotation angle reaches a maximum at an incidence of about 70^0. In the case of normal incidence a direct proportionality of the Kerr angles to the normal component of the magnetization is demonstrated by changing the orientation of the magnetization. When relating Kerr angles as calculated for a set of angles between the surface normal and the orientation of the magnetization to the corresponding magnetic anisotropy energy a very compact description of the occurring reorientation transition can be given. Moreover, based on these data and using a simple phenomenological picture a qualitative description of the Kerr angles with respect to applied external fields is provided.

PACS numbers: 77.22.Ch, 78.20.Bh, 78.20.Ci, 78.20.Ls

Normal & off-normal incidence

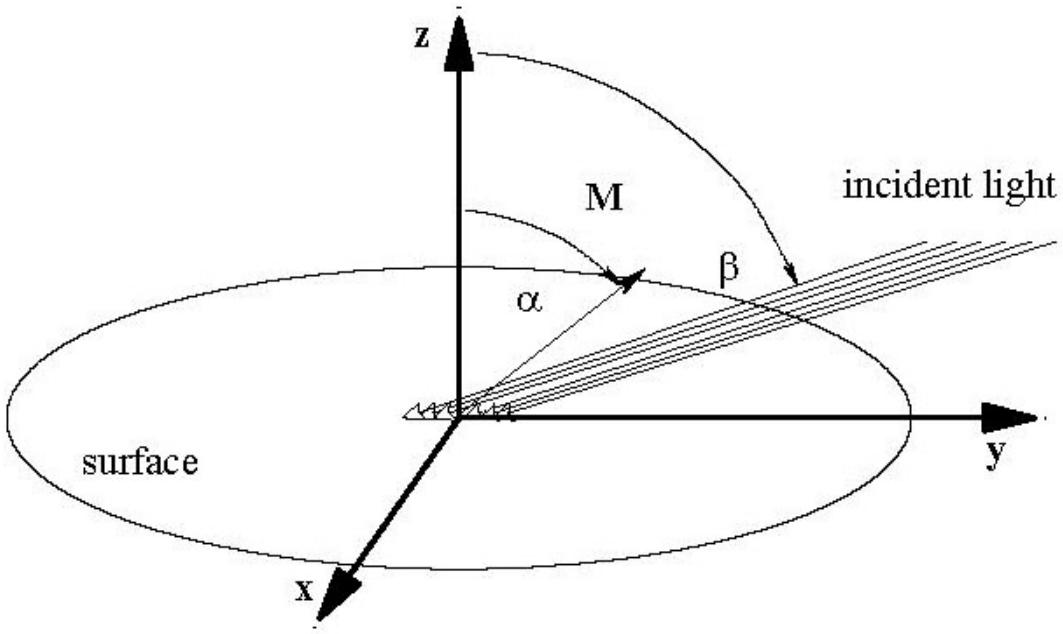

FIG. 1: Kerr set-up used in the calculations in the case of a p-polarized incident light. Here α and β specify the orientation of the magnetization **M** and the direction of the incident light, respectively. Both are specified with respect to the surface normal. Note that the magnetization always lies in the plane of incidence.

CMS

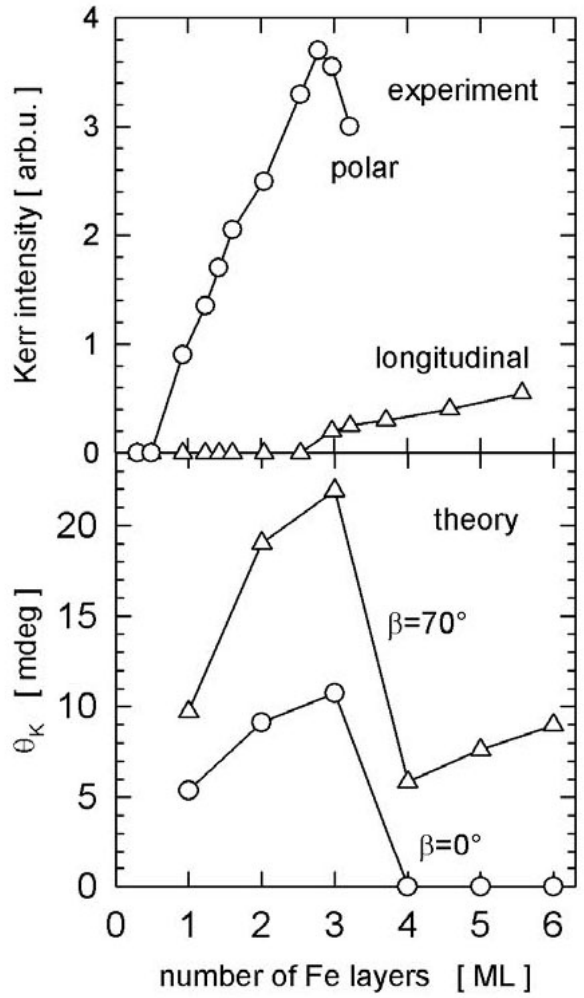

FIG. 2: Top: SMOKE experiments by Liu and Bader [1]. Circles denote the measured data for the polar, whereas triangles for the longitudinal Kerr set-up. Bottom: calculated values of the Kerr rotation angle θ_K in the case of p-polarized incident light and for the magnetic ground state of $Fe_n/Au(100)$. Circles mark the theoretical results for a normal incidence ($\beta = 0^0$) and triangles for an incidence of $\beta = 70^0$, see also Fig. 1.

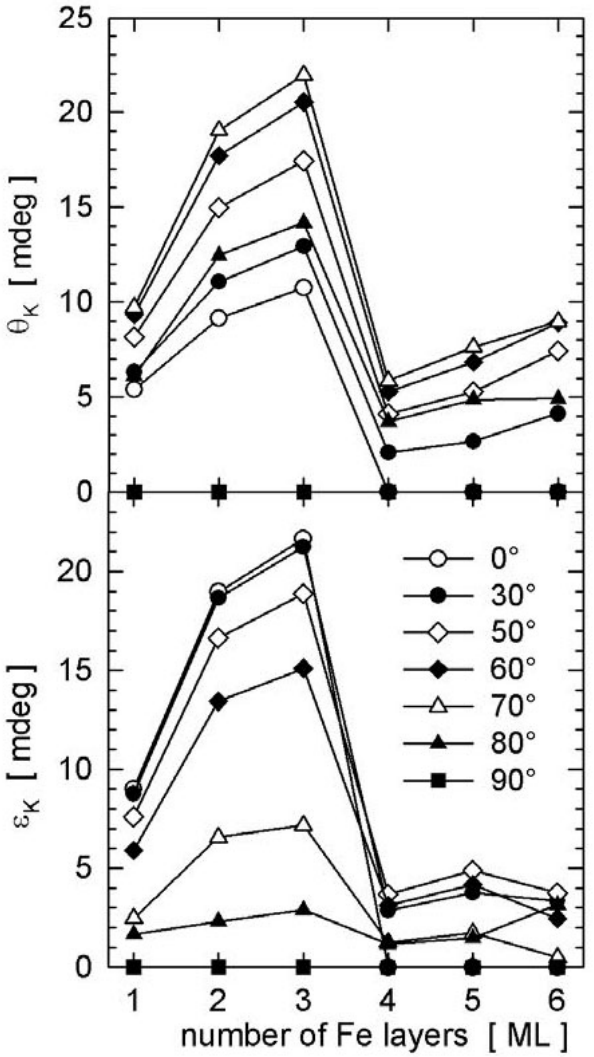

FIG. 3: Calculated Kerr rotation angle (upper part) and ellipticity angle (lower part) for different angles of incidence, see Fig. 1, for the corresponding magnetic ground state of $Fe_n/Au(100)$.

Optimizaton of Kerr angles – a patent based on theory

PHYSICAL REVIEW B **70**, 134411 (2004)

Magneto-optical Kerr effect from layered systems when using elliptically polarized incident light

A. Vernes and P. Weinberger
Center for Computational Materials Science, Technical University Vienna, Gumpendorferstrasse 1a, A-1060 Vienna, Austria
(Received 29 January 2004; revised manuscript received 25 May 2004; published 15 October 2004)

Exploiting the dependence of Kerr spectra on the polarization state of incident light, it is shown that Kerr angles can be optimized by using elliptically polarized incident light. The proposed scheme is applied to fcc Ni(100) and fcc $Co/Pt_3/Co/Pt(100)$. By making use of the complex optical conductivity tensor (calculated by means of the spin-polarized relativistic screened Korringa-Kohn-Rostoker method) and an appropriate 2×2 matrix formalism (to include all reflections and interferences) it is found, that the Kerr angle can be increased substantially even for very small deviations from perfect normal incidence or polar geometry. This increase pertains over the entire visible range of photon energies when using almost circularly polarized incident light. In the case of Ni(100) it is shown that depending on the photon energy even in using arbitrary linearly polarized incident light of azimuth different than ±45°, the Kerr angles can be improved by 5–60 %.

DOI: 10.1103/PhysRevB.70.134411 PACS number(s): 78.20.Bh, 78.20.Ci, 78.20.Ls, 78.67.Pt

The Kerr angle landscape

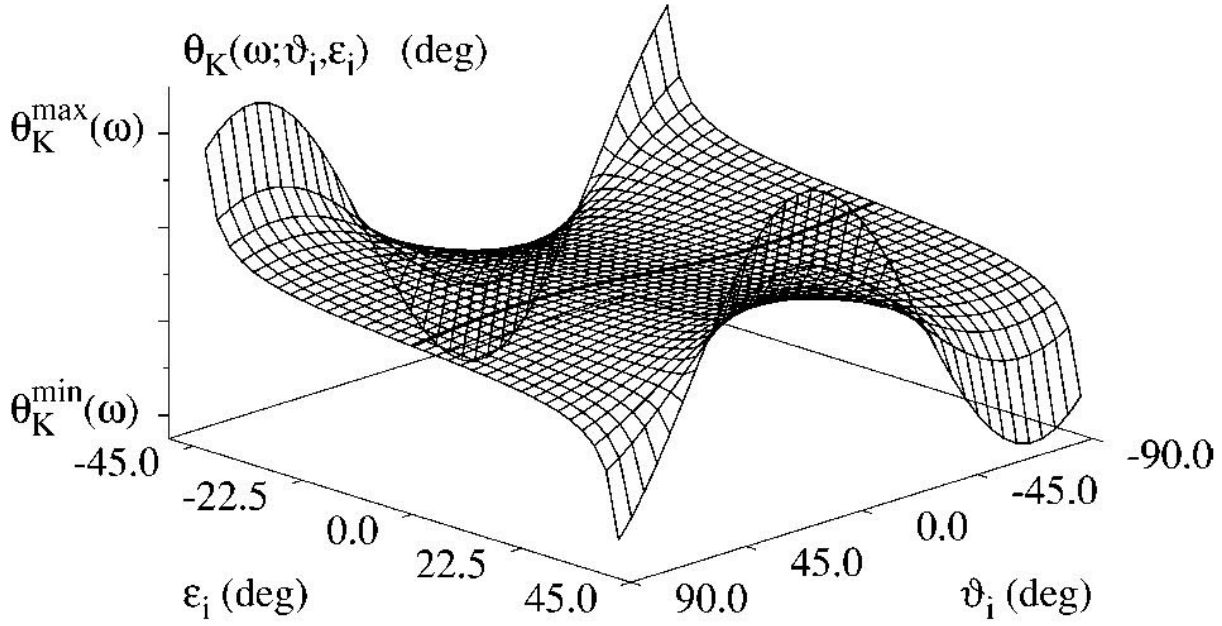

FIG. 2. Polar Kerr angle for almost normal incidence (θ=2°) and arbitrary photon energies ω within the visible spectrum in the case of fcc Ni(100) as a function of the polarization state of the incident light characterized by the azimuth ϑ_i and the ellipticity angle ϵ_i. The solid bold line represents the Kerr angle calculated for arbitrary linearly polarized light (ϵ_i=0). For ω=5 eV, for example, θ_K^{max} is at 0.3° and θ_K^{min} at −0.45°.